Functional Materials 21, No.3 (2014)

Synthesis, characterization and electrical properties of $Pb_{(8-x)}Na_2Nd_x(VO_4)_6O_{(x/2)}$ solid solutions

E.I.Getman, T.M.Savankova, A.V.Ignatov, K.G.Didorenko, A.Y.Talykova, L.I.Ardanova*

Department of Inorganic Chemistry, Donetsk National University, 24 Universitetskaya Str., 83001 Donetsk, Ukraine
*Department of Chemistry and Geology, Minnesota State University, Mankato, 241 Ford Hall, Mankato, 56001 Minnesota, United States

Received March 3, 2014

Substitution of neodymium for lead in the apatite structure in accordance to scheme $2Pb^{2+} + \square \rightarrow 2Nd^{3+} + O^{2-}$ has been investigated by X-ray powder diffraction, scanning electron microscopy, IR spectroscopy and the measurement of electrical conductivity. It was established that single phase solid solutions $Pb_{(8-x)}Na_2Nd_x(VO_4)_6O_{(x/2)}$ are formed in the range of $x = 0–0.25$. The crystal structure features of some samples have been refined by the Rietveld method. It was shown that ions Nd^{3+} preferably occupy M(1) site. Influence of the composition x on the electrical conductivity and activation energy has been investigated.

Методами рентгенофазового анализа, рентгеноструктурного анализа порошка, сканирующей электронной микроскопии, ИК-спектроскопии и измерением электропроводности изучено изоморфное замещение свинца на неодим в структуре апатита в соответствии со схемой замещения $2Pb^{2+} + \square \rightarrow 2Nd^{3+} + O^{2-}$. Установлено, что однофазные твердые растворы состава $Pb_{(8-x)}Na_2Nd_x(VO_4)_6O_{(x/2)}$ образуются в области составов $x = 0–0.25$. Особенности кристаллической структуры некоторых образцов уточнялись с помощью алгоритма Ритвельда. Установлено, что ионы Nd^{3+} преимущественно заселяют позицию M(1) структуры. Изучено влияние степени замещения на электропроводность и энергию активации проводимости твердых растворов.

Синтез, характеристика та електрофізичні властивості твердих розчинів складу $Pb_{(8-x)}Na_2Nd_x(VO_4)_6O_{(x/2)}$. *Є.І.Гетьман, Т.М.Саванкова, О.В.Ігнатов, К.Г.Дідоренко, А.Ю.Таликова, Л.І.Ардanова.*

Методами рентгенофазового аналізу, рентгеноструктурного аналізу порошку, скануючої електронної мікроскопії, ІЧ-спектроскопії та вимірюванням електропровідності досліджено ізоморфне заміщення плюмбуму на неодим у структурі апатиту у відповідності до схеми $2Pb^{2+} + \square \rightarrow 2Nd^{3+} + O^{2-}$. Встановлено, що однофазні тверді розчини складу $Pb_{(8-x)}Na_2Nd_x(VO_4)_6O_{(x/2)}$ утворюються у діапазоні $x = 0–0.25$. Особливості кристалічної структури деяких зразків уточнювалися за допомогою алгоритму Рітвельда. Встановлено, що іони Nd^{3+} переважно локалізуються у позицію M(1) структури. Досліджено вплив ступеню заміщення на електропровідність та енергію активації провідності твердих розчинів.

1. Introduction

Apatites of general formula $M_{10}(ZO_4)_6X_2$ (where M = Na^+, K^+, Ca^{2+}, Sr^{2+}, Ba^{2+}, Pb^{2+}, Cd^{2+}, Eu^{3+}, Y^{3+}, La^{3+}, etc.; Z = Si^{4+}, Ge^{4+}, P^{5+}, V^{5+}, As^{5+}, S^{6+}, Cr^{6+}, etc.; X = OH^-, F^-, Cl^-, Br^-, I^-, O^{2-}, □ — vacancies, etc.) are characterized by different properties. Compounds with apatite structure find an application as bioactive, luminescent and laser materials, sensors, solid electrolytes, adsorbents, catalysts [1–4] and so on. Thus, compounds with apatite structure have been investigated intensively. In terms of crystal chemistry the formula of apatite can be written as $[M(1)]_4[M(2)]_6(ZO_4)_6X_2$. In this structure M ions occupy two structurally nonequivalent positions M(1) and M(2). M(1) site (4*f* position) is occupied by nine atoms of oxygen which also are part of ZO_4 tetrahedra. M(2) site (6*h* position) is occupied by six atoms of oxygen which enter into the composition of ZO_4 tetrahedra and the atom X (2*a* position) located in the channel of the structure. Ions in 6*h* position form triangles. The central axis of these triangles coincides with axis *z*. Repetition of this structure along the axis *z* allows the formation of channels. Ions *X* located in the channel can move along [5].

Compounds with apatite structure can easily accommodate a great variety of substitutions. Substitutions not only make changes in already existing properties, but also cause the emergence of the new ones. Thus, synthesis and investigation of solid solutions based apatite are not only a way to produce novel functional materials with improved physical and chemical characteristics, but also solving the fundamental problem of modern chemistry such as establishment of relationship "composition-structure-property".

Substitutions of rare-earth elements for alkaline-earth elements in the structure of apatite [6–8] have been studied by now. In spite of ionic radii of lead and alkaline-earth elements are similar, the information about substitutions of rare-earth elements for lead in $Pb_{(10-x)}Ln_x(ZO_4)_6(OH)_{(2-x)}O_x$ systems is absent. It's due to the presence of stoichiometric active electron pairs of lead which prevent to substitution by scheme $Pb^{2+} + OH^- \rightarrow Ln^{3+} + O^{2-}$. However, such substitutions in compound $Pb_8Na_2(VO_4)_6$ are possible (similar substitutions were investigated in $Pb_8Na_2(PO_4)_6$ [9]) because of OH^- groups which are absent in its structure and this compound has less electron pairs as compared with the compound $Pb_{10}(VO_4)_6(OH)_2$.

Considerably lower synthesis temperature is the advantage of the system based on lead-sodium apatite [10, 11] as compared with apatite of alkaline-earth elements [6]. This fact simplifies the technique of synthesis and promotes obtaining fine-dispersed grains. Furthermore, the channels of the structure of these compounds are empty. This favors the conduction of oxygen in case of realization the foregoing scheme. Therefore, the purpose of this study is to investigate substitution of neodymium for lead in the structure of $Pb_8Na_2(VO_4)_6$ compound.

2. Experimental

Samples of $Pb_{(8-x)}Na_2Nd_x(VO_4)_6O_{(x/2)}$ were prepared from mixtures of lead oxide PbO (99.0 % purity), neodymium oxide Nd_2O_3 (99.0 % purity), sodium carbonate Na_2CO_3 (99.8 % purity) and ammonium vanadate NH_4VO_3 (99.0 % purity) which were composed stoichiometry for $x = 0$, 0.05, 0.10, 0.15, 0.20, 0.25, 0.30, 0.40, 0.50 and 0.60. The mixtures were homogenized in an agate mortar for 20 min, placed in alumina crucibles and calcined at 300 and 500°C for 1 h at each temperature. After that the mixtures were heated up to 600°C for 5–6 h. After sintering the samples were powdered and analyzed by X-ray powder diffraction. Then the samples were sintered again. This step was repeated several times until a constant phase composition was obtained. Total time of sintering at 600°C came to 67 h.

X-ray powder diffraction patterns of the samples were recorded at room temperature, using a powder diffractometer DRON-3M with Ni-filtered copper K_α radiation. The scanning rate was 2°/min, Si was used as an external standard. Parameters *a* and *c* of the hexagonal unit cell of apatite were calculated from the positions of the 16 most intense and sharp reflections by using a least refinement program. The X-ray powder diffraction data for crystal structure refinement was collected in the step regime: step 0.05° (2Θ), interval $15.00 \leq 2\Theta \leq 140°$, scanning rate 3 s per step. The crystal structure was refined using program FULLPROF.2k (version 3.40) [12] with graphic interface WinPLOTR [13]. Factors of veracity R_B, R_F, R_P, R_{WP} and χ^2 are 7.86, 6.88, 7.85, 10.1, 1.63 for composition $x = 0$ and 5.03, 5.02, 6.37, 8.30, 1.34 for composition with $x = 0.2$.

IR spectra of the samples dispersed in KBr tablets (pressure 700 MPa) were recorded using Bruker-Optics Fourier trans-

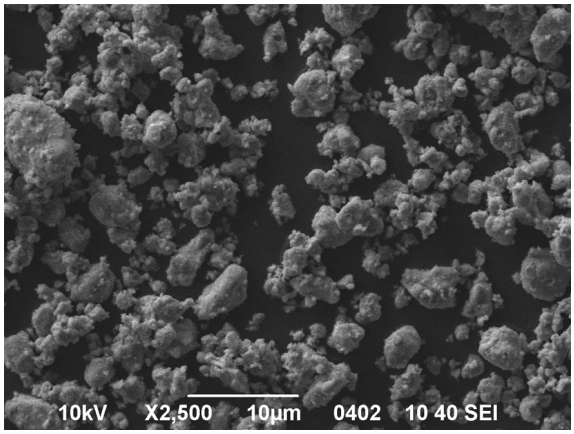

Fig. 1. Microphotography of $Pb_{7.75}Na_2Nd_{0.25}(VO_4)_6O_{0.125}$ sample (zooming in 2.500).

form infrared spectrophotometer in the range of 400–40000 cm^{-1}.

Elemental analysis was performed using JEOL JSM-6490LV SEM with INCA Penta FETx3 (OXFORD Instruments) energy dispersion spectrometer. The micrographs and element distribution maps over the surface of the samples were also obtained using this instrument.

Electrical conductivity measurements were performed using DE-5000 LCR-meter at frequency 100 kHz in the range of 300–600°C with heating rate 2°/min. The powders of single phase solid solutions were pressed under 120 MPa (diameter 0.8 cm) and sintered at 600°C during 70 h for electrical conductivity measurements. Electrodes were deposited as silver paste. The applied signal frequency was 100 kHz.

3. Results and discussion

The sample of $Pb_{7.75}Na_2Nd_{0.25}(VO_4)_6O_{0.125}$ was investigated using scanning electron microscopy. Fine powder was obtained from the synthesis; the size of aggregates was 3–5 μm, and the grains' size was 1 μm (Fig. 1). Electron microscopy reveals (Fig. 2) that the elements are distributed over the particle surface almost uniformly, which indicates formation of the homogeneous sample. The residual nonuniformity is due to the surface pattern.

Elemental composition was determined over 14 points (surface regions) for compositions $x = 0$ and 0.25 (Table 1). The error of determination of element content is com-

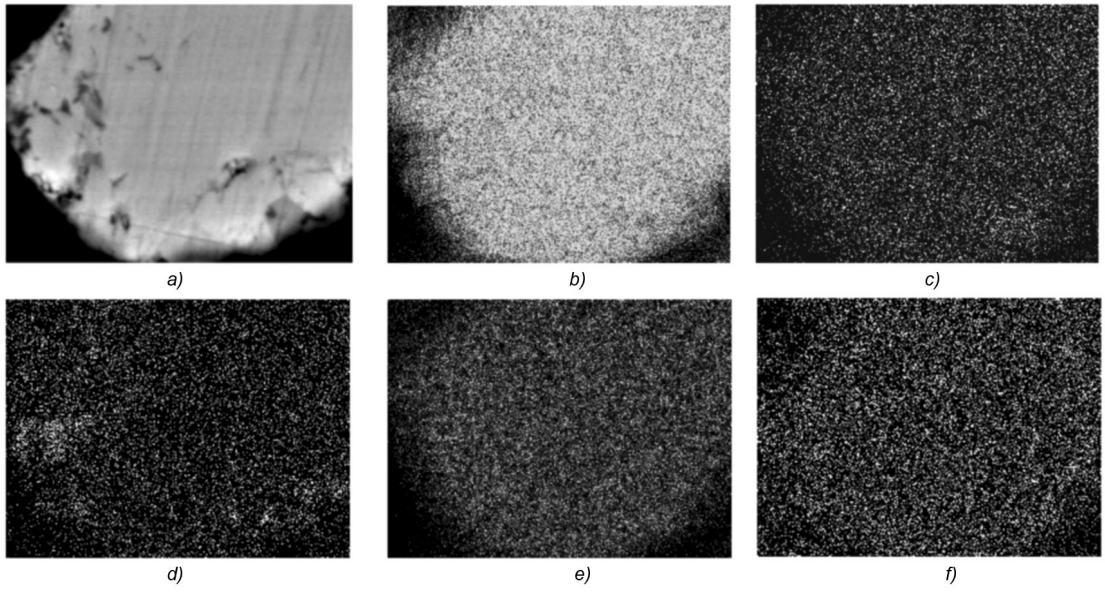

Fig. 2. Microphotography of $Pb_{7.75}Na_2Nd_{0.25}(VO_4)_6O_{0.125}$ sample (a) and distribution of elements: lead (b), sodium (c), neodymium (d), vanadium (e), oxygen (f).

Table 1. Results of elemental analysis for the samples $Pb_{(8-x)}Na_2Nd_x(VO_4)_6O_{(x/2)}$ (mass. %)

x	V		Pb		Nd		Na		O	
	exper.	theor.	exper.	theor.	exper.	theor.	exper.	theor.	exper.	theor.
0	13.62	12.77	69.99	69.26	–	–	1.93	1.92	14.46	16.05
0.25	14.32	12.85	68.93	67.49	1.91	1.52	1.77	1.93	13.06	16.21

Table 2. Unit cell parameters for the samples $Pb_{(8-x)}Na_2Nd_x(VO_4)_6O_{(x/2)}$

Composition, x	a (Å)	c (Å)
0	10.0569±0.0012	7.3265±0.0011
0.05	10.0534±0.0014	7.3272±0.0014
0.10	10.0499±0.0012	7.3262±0.0012
0.15	10.0466±0.0010	7.3230±0.0010
0.20	10.0415±0.0013	7.3232±0.0014
0.25	10.0396±0.0015	7.3209±0.0015

parable with the data obtained in [14] for compounds with apatite structure using the same method of research. It indicates that lead oxide has not undergone sublimation during the apatite synthesis.

The peaks in X-ray diffraction patterns of the samples with $x = 0–0.25$ are sharp and well resolved and can be attributed to hexagonal crystal form of apatite (Fig. 3). The diffraction patterns of the samples with $x > 0.25$ also contain reflections of neodymium vanadate $NdVO_4$. The intensity of these reflections increases with increase of neodymium content. Thus, it was established by X-ray powder diffraction that the limit for substitution of neodymium for lead in the structure of apatite is in the range of $0 \le x \le 0.25$.

The lattice parameters of the hexagonal unit cell are presented in Table 2. The unit cell parameter a of the hexagonal lattice decreases slightly, while the parameter c remains almost unchanged of single-phase samples with increasing neodymium content in solid solution. It is due to smaller ionic radius of neodymium Nd^{3+} (1.163 Å) compared to the radius of lead Pb^{2+} (1.350 Å). Here and below the ionic radii are presented according to R. Shennon [15] for coordination number 9. However, such a small change needs to be explained, since the difference between the ionic radii is considerable (0.187 Å).

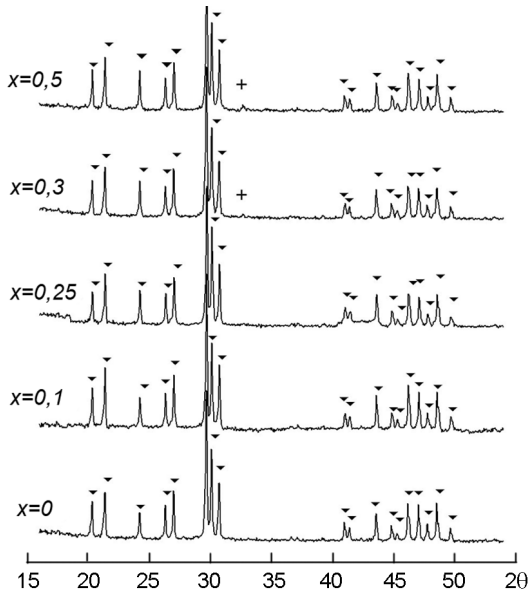

Fig. 3. Diffractograms of $Pb_{(8-x)}Na_2Nd_x(VO_4)_6O_{(x/2)}$ samples (— apatite structure phase, + — phase of $NdVO_4$).

The unit cell parameters of apatites such as $Pb_{10}(VO_4)_6(OH)_2$, $Na_2Pb_8(VO_4)_6$ and $K_2Pb_8(VO_4)_6$ are presented in Table 3 for explanation of the reasons for such change. It is seen that substitution of alkali metals for lead reduce to significant decrease of parameters not only in the case of sodium, but in the case of potassium although the radius of ion K^+ (1.550 Å) is bigger than the ionic radius of the ion Pb^{2+} (1.350 Å).

Entry to $Pb_{10}(VO_4)_6(OH)_2$ structure of alkaline metals reduces the size of the cells of apatite so much that the partial substitution of neodymium for lead doesn't influence on the values of parameters.

The refinement results indicate that sodium substitute for lead mainly in M(1) positions according to [17–20]. Fourfold M(1) position contains 41.5 % sodium and 58.5 % lead, while sixfold M(2) position

Table 3. Unit cell parameters for some apatites

Composition	a (Å)	c (Å)	Reference
$Pb_{10}(VO_4)_6(OH)_2$	10.2242(3)	7.4537(3)	[15]
$Na_2Pb_8(VO_4)_6$	10.060(2)	7.346(1)	[16]
$Na_2Pb_8(VO_4)_6$	10.059(3)	7.434(2)	[11]
$K_2Pb_8(VO_4)_6$	10.111(2)	7.448(1)	[16]
$Na_2Pb_8(VO_4)_6$	10.057(1)	7.327(1)	This article

Table 4. Interatomic distances (Å in the structure of $Pb_{(8-x)}Na_2Nd_x(VO_4)_6O_{(x/2)}$

Composition	$x = 0$	$x = 0.2$
Pb(1)–O(1) x 3	2.44(3)	2.46(3)
Pb(1)–O(2) x 3	2.82(3)	2.75(3)
Pb(1)–O(3) x 3	2.98(3)	3.02(2)
<Pb(1)–O>	2.75(1)	2.74(1)
Pb(2)–O(1)	2.71(4)	2.81(3)
Pb(2)–O(2)	2.30(4)	2.26(4)
Pb(2)–O(3) x 2	2.62(3)	2.70(3)
Pb(2)–O(3) x 2	2.48(2)	2.55(2)
<Pb(2)–O(1-3)>	2.54(1)	2.60(1)
Pb(2)–(4)	–	2.533(4)
Pb(2)–Pb(2)	4.405(7)	4.387(7)

contains 5.7 % sodium and 94.3 % lead. On the assumption of this fact we considered that sodium substitute for lead mainly in the M(1) positions during refinement of the crystal structure $Pb_{(8-x)}Na_2Nd_x(VO_4)_6O_{(x/2)}$. The refinement of the crystal structure of $Pb_{7.8}Na_2Nd_{0.2}(VO_4)_6O_{0.1}$ showed that the M(1) position contains 41.5 % sodium, 54.0 % — lead, 4.5 % — neodymium, while the M(2) position contains 5.7 % sodium, 94.0 % — lead, and 0.3 % — neodymium. Thus, neodymium substitute for lead mainly in the M(1) positions. Obtained values of atomic coordinates enable calculation of the interatomic distances; some of them are given in Table 4. As can be seen the values of average interatomic distances are changed insignificantly. A little increasing of distance Pb(2)–O(1-3) from 2.54(1) to 2.60(1) and decreasing of distance Pb(2)–Pb(2) from 4.405(7) to 4.387(7) Å can be explained by appearance of oxygen ions in the structure channels. It increases the coordination number of lead ions Pb(2) from 6 to 7 which results in increasing its dimensions. In addition oxygen ions located in the channels react with lead ions Pb(2). Because of this fact the distance between Pb(2)–Pb(2) decreases.

The cause of slight change of the both unit cell parameters and interatomic distances should be searched in the electronic structure of lead atom. Impossibility of substitution in $Pb_{(10-x)Lnx}(ZO_4)_6(OH)_{(2-x)}O_x$ systems has the same explanation. Lead apatite $Pb_{10}(ZO_4)_6(OH)_2$ has OH^- groups located in the structure channels and stoichiometric active electron pairs. Concentration of the both OH^- groups and electron pairs is reduced during the substitution according to $Pb^{2+} + OH^- \rightarrow Na^+ + \square$. It results in compaction of the structure. Indeed, the values of Pb–O distances are 2.210 and 2.218 Å for vanadates $Pb_8Na_2(VO_4)_6$ and $Pb_8K_2(VO_4)_6$, respectively [17], while the value of Pb–O distance for $Pb_{10}(VO_4)_6(OH)_2$ is 2.35 Å [21]. Thus, character of the chemical bond has determining the influence in this case.

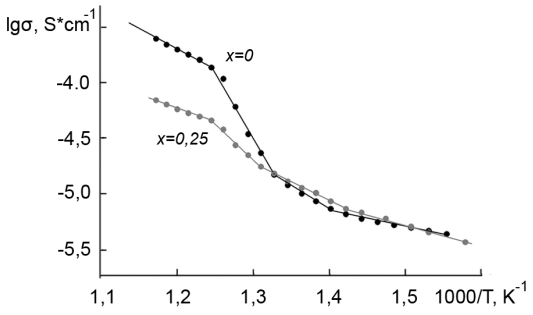

Fig. 4. Logarithm of conductivity, lgσ (S cm^{-1}) as a function of $1000/T$ (K^{-1}) for $Pb_{(8-x)}Na_2Nd_x(VO_4)_6O_{(x/2)}$.

IR spectra for compound $Pb_8Na_2(VO_4)_6$ and solid solution $Pb_{7.75}Na_2Nd_{0.25}(VO_4)_6O_{0.125}$ have been investigated. For $Pb_8Na_2(VO_4)_6$ the lines observed at 760, 819, 845 and 416, 466 and 514 cm^{-1} correspond to stretching ν_3 (VO_4) and ν_4 (VO_4), respectively [11, 21, 22]. Frequency of lines ν_4 and ν_3 (819 cm^{-1}) are increasing by 3–5 cm^{-1} and 2 cm^{-1} respectively during the substitution of neodymium for lead. Furthermore, the spectrum of $Pb_{7.75}Na_2Nd_{0.25}(VO_4)_6O_{0.125}$ solid solution has an additional band at 444 cm^{-1}. However, additional bands were found during the investigation of substitution in $Ca_{(10-x)}La_x(PO_4)_6(OH)_y$ [6] and $Sr_{(10-x)}Eu_x(PO_4)_6(OH)_{(2-x)}O_x$ [22] systems. These bands were attributed to vibrations of La–O and Eu–O, respectively. Therefore, the band at 444 cm^{-1} can be attributed to the vibrations of Nd–O.

Temperature dependences of conductivity are presented in Fig. 4 for compositions $x = 0$ and 0.25. Only one linear segment was obtained in [11] for $Pb_8Na_2(VO_4)_6$ in the temperature range of 350–456°C. In our work the conductivity was defined in the temperature range of 300–600°C. Four linear segments were obtained with activation energies of 0.49, 1.61, 4.84 and 1.41 eV in the temperature ranges of 300–440, 440–480, 480–530 and 530–600°C, respectively

Table 5. Activation energy (eV) for the samples $Pb_{(8-x)}Na_2Nd_x(VO_4)_6O_{(x/2)}$

$x = 0$	$x = 0.05$	$x = 0.1$	$x = 0.15$	$x = 0.2$	$x = 0.25$
0.49 (300–440°C)*	0.50	0.62	0.64	0.61	0.67
1.61 (440–480°C)*	0.58	1.11	1.14	1.20	1.26
4.84 (480–530°C)*	2.92	2.97	2.96	2.91	2.57
1.41 (530–600°C)*	2.89	2.76	2.27	1.30	0.99

* Temperature intervals are presented for $Pb_8Na_2(VO_4)_6$. Everything else has similar values.

Table 6. Conductivity (S,cm^{-1}) and relative density (ρ, %) for the samples $Pb_{(8-x)}Na_2Nd_x(VO_4)_6O_{(x/2)}$

x	350°C	400°C	450°C	500°C	550°C	600°C	ρ, %
0	$0.38\cdot10^{-5}$	$0.52\cdot10^{-5}$	$0.86\cdot10^{-5}$	$2.5\cdot10^{-5}$	$17\cdot10^{-5}$	$30\cdot10^{-5}$	94
0.05	$0.12\cdot10^{-5}$	$0.16\cdot10^{-5}$	$0.22\cdot10^{-5}$	$0.63\cdot10^{-5}$	$1.9\cdot10^{-5}$	$3.7\cdot10^{-5}$	94
0.10	$0.17\cdot10^{-5}$	$0.19\cdot10^{-5}$	$0.29\cdot10^{-5}$	$0.69\cdot10^{-5}$	$2.4\cdot10^{-5}$	$5.1\cdot10^{-5}$	94
0.15	$0.22\cdot10^{-5}$	$0.34\cdot10^{-5}$	$0.55\cdot10^{-5}$	$1.0\cdot10^{-5}$	$3.8\cdot10^{-5}$	$9.5\cdot10^{-5}$	95
0.20	$0.29\cdot10^{-5}$	$0.49\cdot10^{-5}$	$0.80\cdot10^{-5}$	$1.5\cdot10^{-5}$	$4.2\cdot10^{-5}$	$9.7\cdot10^{-5}$	94
0.25	$0.35\cdot10^{-5}$	$0.60\cdot10^{-5}$	$1.0\cdot10^{-5}$	$2.2\cdot10^{-5}$	$5.3\cdot10^{-5}$	$10\cdot10^{-5}$	95

(Table 5). The values of activation energy and electrical conductivity (Table 6) unmodified $Pb_8Na_2(VO_4)_6$ in the temperature range of 300–440°C (activation energy of 0.59 eV, conductivity $0.37\cdot10^{-5}$, $0.67\cdot10^{-5}$ and $1.30\cdot10^{-5}$ at 350, 400 and 450°C) agree with [11]. In the temperature ranges of 440–480 and 530–600°C activation energies are 1.61 and 1.41 eV, respectively, which enter the range of 1.21–2.07 eV for $Pb_8K_{(2-x)}Na_x(PO_4)_6$ also having cationic conductivity [23].

However, the value of activation energy for $Pb_8Na_2(VO_4)_6$ is very high in the temperature range of 480–530°C (4.84 eV), which is not typical for ionic conductivity. Similar activation energy (3.85 eV) and temperature dependence of the conductivity are obtained for compound with the apatite structure $Pb_{4.8}Bi_{1.6}Na_{3.6}(PO_4)_6$ [24]. High value of activation energy was explained using the Rietveld analysis. Authors established that sodium atoms initially localized in (6*h*) site, are found in the center of the tunnel at 900 K. Herewith $Pb_{4.8}Bi_{1.6}Na_{3.6}(PO_4)_6$ has cationic conductivity throughout the temperature range.

The value of activation energy depends on the both composition x and temperature. In the temperature range of 300–440°C the activation energy increases insignificantly with increasing of x (Table 5). In the temperature range of 440–480°C the activation energy decreases considerably from 1.61 to 0.58 eV, where upon it increases gradually

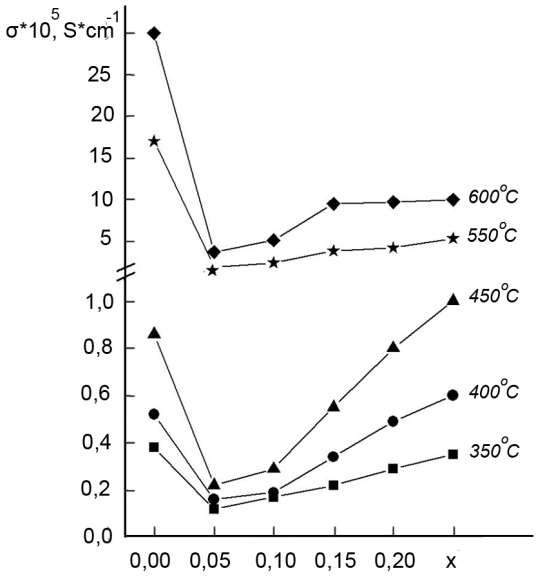

Fig. 5. Conductivity of $Pb_{(8-x)}Na_2Nd_x(VO_4)_6O_{(x/2)}$ samples as a function of x at different temperatures.

to 1.26 eV. In the temperature range of 530–600°C the activation energy increases considerably from 1.41 to 2.89 eV, whereupon it decreases gradually to 0.99 eV. In spite of decreasing of the activation energy from 4.84 to 2.57 eV in the temperature range of 480–530°C, its value is maximum for each composition. It is evidence of relocation of sodium in tunnel of structure not only for

$Pb_8Na_2(VO_4)_6$ but also for solid solutions of $Pb_{(8-x)}Na_2Nd_x(VO_4)_6O_{(x/2)}$.

In the beginning (for $x = 0.05$) the conductivity decreases considerably, but after that it increases gradually with increasing the composition x (Table 6, Fig. 5). At the temperature 400–450°C the conductivity for $x = 0.25$ is greater than for $Pb_8Na_2(VO_4)_6$, however it is less at more high temperature. Foregoing dynamics of change of the activation energy and conductivity is needed of explanation.

It is known that a kind of conductivity depends on chemical composition. Thus, compounds $Ca_{10}(PO_4)_6(OH)_2$ and $Ca_{9.5}Na_{0.5}(PO_4)_6(OH)_{1.5}$ have protonic conductivity, compound $Ca_{8.5}La_{1.5}(VO_4)_6O_{1.75}$ has anionic conductivity (O^{-2}), compound $Pb_8K_2(VO_4)_6$ has cationic conductivity (K^{+1}) [25], compound $Pb_{10}(PO_4)_6(OH)_2$ has mixed conductivity (e^- and OH^-) [26]. The kinds of ionic conductivity are cationic, anionic or mixed [27, 28].

Compound $Pb_8Na_2(VO_4)_6$ has cationic conductivity because of movement of alkali metal cation along the structure channels. In consideration of scheme of substitution $2Pb^{2+} + \square \rightarrow 2Nd^{3+} + O^{2-}$ emergent oxygen ions are located in the channels of the structure. These ions block partially transfer of sodium ions in the channels and their movement along the structure channel. Consequently cationic conductivity decreases considerably at $x = 0.05$ and anionic part of the conductivity appears. The value of anionic conductivity increases with the rise of neodymium content.

4. Conclusions

Solid solutions $Pb_{(8-x)}Na_2Nd_x(VO_4)_6O_{(x/2)}$ have been investigated using X-ray diffraction, refinement of crystal structure by the Rietveld method, scanning electron microscopy, IR-spectroscopy and measurement of electrical conductivity. Substitution of neodymium for lead corresponded to the scheme $2Pb^{2+} + \square \rightarrow 2Nd^{3+} + O^{2-}$ as been carried out in range of homogeneity $0 \le x \le 0.25$. Dynamics of change of activation energy and conductivity are the reason for transition from cationic conductivity to mixed cationic and anionic conductivity.

References

1. D.Grossin, S.Rollin-Martinet, C.Estournes et al., *Acta Biomaterialia*, **6**, 577 (2010).
2. J.Zhang, H.Liang, R.Yu et al., *Mater. Chem. and Phys.*, **114**, 242 (2009).
3. H.Yoshioka, Y.Nojiri, S.Tanase, *Solid State Ionics*, **179**, 2165 (2008).
4. S.Kale, S.Kahandal, S.Disale et al., *Current Chemistry Letters*, **1**, 69 (2012).
5. U.Breg, G.Klaringbull, Kristallicheskaya struktura mineralov. M.: Mir, 1967. [in Russian]
6. A.Serret, M.V.Cabanas, M.Vallet_Regi, *Chem. Mater.*, **12**, 3836 (2000).
7. E.Get'man, N.Yablochkova, S.Loboda et al., *J. Solid State Chem.*, **181**, 264 (2008).
8. L.Ardanova, E.Get'man, S.Loboda et al., *Inorg. Chem.*, **49**, 10687 (2010).
9. L.Brixner, P.Bierstedt, *J. Solid State Chem.*, **13**, 24 (1975).
10. R.Verbeeck, C.Lassuyt, H.Heijligers et al., *Calcified Tissue Intern.*, **33**, 243 (1981).
11. E.Chakroun-Ouadhour, R.Ternare, D.Ben Hassen-Chehimi et al., *Mater. Res. Bull.*, **43**, 2451 (2008).
12. C.J.Rodriguez, Program FullProf. 2k, version 3. 40.LLB JRC (unpublished), November 2005.
13. D.Arcos, J.Rodriguez-Carvajal, M.Vallet-Regi, *Chem. Mater.*, **17**, 57 (2005).
14. R.D.Shannon, *Acta Crystallographica*, **32**, 751 (1976).
15. M.Mathew, W.Brown, M.Austin et al., *J. Solid State Chem.*, **35**, 69 (1980).
16. Mohamed Azrour, Lahcen El Ammari, Yvette Le Fur et al., *J. Solid State Chem.*, **141**, 373 (1998).
17. E.Getman, A.Ignatov, S.Loboda, *Ukrainian Chem. J.*, **77**, 10 (2011).
18. Mohamed Toumi, *J. Ceramic Soc. Japan*, **116**, 904 (2008).
19. M.Elkoumiri, S.Oishi, S.Sato et al., *Mater. Res. Bull.*, **35**, 503 (2000).
20. J.G.Eon, C.B.Boechat, A.M.Rossi et al., *Phys. Chem. Chem. Phys.*, **8**, 1845 (2006).
21. C.B.Boechat, J.G.Eon, A.M.Rossi et al., *Phys. Chem. Chem. Phys.*, **2**, 4225 (2000).
22. J.-L.Lacout, A.Taitai, G.Bonel, *Compt. Rendus de L'Academ. Scie.*, **304**, 699 (1987).
23. A.Laghzizil, Ph.Barboux, A.Bouhaouss, *Solid State Ionics*, **128**, 177 (2000).
24. B.Hamdi, H.El Feki, A.Ben Salah et al., *Solid State Ionics*, **177**, 1413 (2006).
25. W.Gao, These de Doctoral, 18 Septembre 2008.
26. T.Takahashi, S.Tanase, O.Yamamoto, *Electrochim. Acta*, **23**, 369 (1978).
27. N.V.Korovin, Electrochemical Energetics, Energoatom, Moscow (1991) [in Russian].
28. F.F.Volkenshtein, Electronic Processes in the Real Crystals. Success. Phys. Scie., **XXVIII**, (1946).